

# Magnetic properties of superconducting FeSe in the normal state

G E Grechnev<sup>1</sup>, A S Panfilov<sup>1</sup>, V A Desnenko<sup>1</sup>, A V Fedorchenko<sup>1</sup>,  
S L Gnatchenko<sup>1</sup>, D A Chareev<sup>2</sup>, O S Volkova<sup>3</sup> and A N Vasiliev<sup>3</sup>

<sup>1</sup> B Verkin Institute for Low Temperature Physics and Engineering, National Academy of Sciences of Ukraine, 61103 Kharkov, Ukraine

<sup>2</sup> Institute of Experimental Mineralogy, Russian Academy of Sciences, Chernogolovka, Moscow Region 142432, Russia

<sup>3</sup> Low Temperature Physics and Superconductivity Department, Department of Physics, Moscow State University, Moscow 119991, Russia

E-mail: grechnev@ilt.kharkov.ua

Received 4 October 2012, in final form 15 November 2012

Published 13 December 2012

Online at [stacks.iop.org/JPhysCM/25/046004](http://stacks.iop.org/JPhysCM/25/046004)

## Abstract

A detailed magnetization study for the novel FeSe superconductor is carried out to investigate the behavior of the intrinsic magnetic susceptibility  $\chi$  in the normal state with temperature and under hydrostatic pressure. The temperature dependences of  $\chi$  and its anisotropy  $\Delta\chi = \chi_{\parallel} - \chi_{\perp}$  are measured for FeSe single crystals in the temperature range 4.2–300 K, and a substantial growth of susceptibility with temperature is revealed. The observed anisotropy  $\Delta\chi$  is very large and comparable to the averaged susceptibility at low temperatures. For a polycrystalline sample of FeSe, the significant pressure effect on  $\chi$  is determined to be essentially dependent on temperature. *Ab initio* calculations of the pressure-dependent electronic structure and magnetic susceptibility indicate that FeSe is close to magnetic instability, with dominating enhanced spin paramagnetism. The calculated paramagnetic susceptibility exhibits a strong dependence on the unit cell volume and especially on the height  $Z$  of chalcogen species from the Fe plane. The change of  $Z$  under pressure determines a large positive pressure effect on  $\chi$ , which is observed at low temperatures. It is shown that the literature experimental data on the strong and nonmonotonic pressure dependence of the superconducting transition temperature in FeSe correlate qualitatively with the calculated behavior of the density of electronic states at the Fermi level.

## 1. Introduction

Soon after the discovery of superconductivity in LaFeAsO<sub>1-x</sub>F<sub>y</sub>, superconductivity was also detected in the binary compound FeSe<sub>1-x</sub> [1] with a transition temperature  $T_c \simeq 8$  K. This compound possesses the simplest crystal structure among the new families of Fe-based superconductors, and consists of a stack of Fe square planar layers, which are tetrahedrally coordinated by Se atoms. Also the large pressure effect on the transition temperature was later observed [2–4] with  $T_c \approx 37$  K at pressures  $P \approx 9$  GPa, indicating that FeSe<sub>1-x</sub> is actually a high-temperature superconductor. Therefore, the superconducting FeSe<sub>1-x</sub> compound has attracted considerable attention and has been a subject of intensive studies for a number of years [5–12]. The structural simplicity of FeSe favors experimental and theoretical studies of chemical substitution and high-pressure effects, which are

aimed at promoting a better understanding of the mechanism of the superconductivity.

Upon cooling below room temperature, the tetragonal  $P4/nmm$  phase of FeSe<sub>1-x</sub> undergoes a subtle distortion to the lower symmetry orthorhombic  $Cmma$  phase [3, 5–7]. This transition occurs within a broad temperature range, about 70–100 K, depending on the stoichiometry of the samples. It was also found that the tetragonal phase undergoes structural transitions under high pressures ( $P \geq 10$  GPa) to the hexagonal non-superconducting  $P6_3mmc$  NiAs-type phase [2, 3, 5], and then to its orthorhombic modification ( $Pbnm$ , MnP-type) [2, 13, 14]. The recent theoretical examination of stability regions of the high-pressure phases of FeSe<sub>1-x</sub> [15, 16] indicated a possibility of metallization and superconductivity in the orthorhombic  $Pbnm$  phase under high pressure.

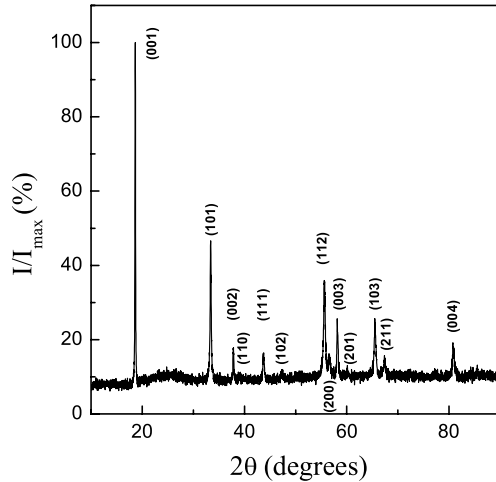


**Figure 1.** The x-ray diffraction pattern of FeSe collected at room temperature (Co  $K\alpha$ -radiation, Fe filter,  $\lambda = 1.79021 \text{ \AA}$ ). The powder samples were prepared by grinding small and medium single crystals in an agate mortar in acetone. All peaks in x-ray diffraction pattern of the ground powder are ascribed to the tetragonal  $P4/nmm$  (129) space group.

For iron-based superconductors, including  $\text{FeSe}_{1-x}$ , a matter of debate is the relationship between superconductivity and magnetism. Though a substantial increase of  $T_c$  under pressure was clearly observed in  $\text{FeSe}_{1-x}$  [2, 3, 17–19], these studies did not detect any magnetic ordering. However, recent NMR studies provided some indication of an incipient magnetic phase transition under pressure [20]. Recently, a static magnetic ordering has been detected above  $P \sim 1 \text{ GPa}$  by means of zero-field muon spin rotation (ZF  $\mu\text{SR}$ ) [21, 22] and neutron diffraction [22]. These studies have revealed that as soon as magnetic ordering emerges, the magnetic and superconducting states apparently coexist, and both the magnetic ordering temperature  $T_N$  and  $T_c$  increase simultaneously with increasing pressure. Also, it was recently found that upon applying pressure the increase of  $T_c$  in  $\text{FeSe}_{1-x}$  appeared to be nonmonotonic and exhibits a local maximum at  $P \simeq 0.8 \text{ GPa}$ , which is followed by a local minimum at  $P \sim 1.2 \text{ GPa}$  [17, 18, 21, 22]. Therefore, there is still a considerable controversy regarding the interplay between the electronic structure, magnetism and superconductivity in the  $\text{FeSe}_{1-x}$  compounds, especially under pressure.

The experimental data on the magnetic susceptibility of the  $\text{FeSe}_{1-x}$  system in the normal state are incomplete and contradictory [8, 12]. Also, these data are mostly obtained on polycrystalline samples and often distorted by the presence of secondary magnetic phases of iron. In order to shed more light on the relationship between magnetic and superconducting properties it is very important to elucidate the intrinsic susceptibility of  $\text{FeSe}_{1-x}$  superconductors and investigate its evolution with doping, temperature, and pressure. Here we report on results of the experimental studies of magnetic properties for single-crystal and polycrystalline FeSe samples of high quality in the normal state. These studies include measurements of the temperature

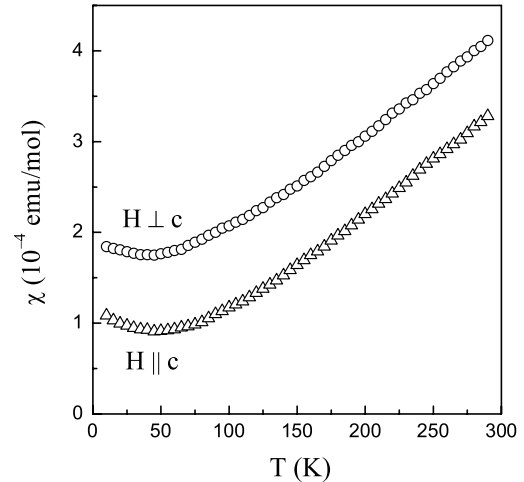


**Figure 2.** Temperature dependence of the magnetic susceptibility in the normal state for the single-crystal FeSe measured in the field  $H = 50 \text{ mT}$ . Data corresponding to the magnetic field directions  $H \perp c$  axis and  $H \parallel c$  are denoted by  $\circ$  and  $\triangle$  symbols, respectively.

dependence of magnetic susceptibility and its anisotropy as well as the hydrostatic pressure effects. The experimental investigations are supplemented by *ab initio* calculations of the electronic structure and magnetic susceptibility of FeSe. The calculations are based on the local-spin-density approximation (LSDA) of density functional theory (DFT). The results of experiments and calculations are used to analyze the nature of magnetism in FeSe and the basic mechanisms of its strong pressure dependence.

## 2. Experimental details and results

The plate-like single crystals of  $\text{FeSe}_{1-x}$  superconductor were grown in evacuated quartz ampules using the  $\text{KCl}/\text{AlCl}_3$  flux technique with a constant temperature gradient of  $5^\circ\text{C cm}^{-1}$  along the ampule length (the temperature of the hot end was kept at  $427^\circ\text{C}$  and the temperature of the cold end was about  $380^\circ\text{C}$ ). Typical dimensions of the produced single-crystal samples are  $(2\text{--}3) \times (2\text{--}3) \times (0.3\text{--}0.5) \text{ mm}^3$ . The tetragonal  $P4/nmm$  structure was demonstrated at room temperature by an x-ray diffraction technique (see figure 1). Energy dispersive x-ray spectroscopy, performed on a CAMECA SX100 (15 keV) analytical scanning electron microscope, revealed an  $\text{Fe}:\text{Se} = 1:0.96 \pm 0.02$  composition, denoted in the following as FeSe for simplicity. This composition corresponds to a region of the tetragonal structure, according to the published Fe–Se phase diagram [23, 24].

The study of the magnetic properties of FeSe samples at ambient pressure was carried out at  $T = 4.2\text{--}300 \text{ K}$  using a SQUID magnetometer. The superconducting transition was detected within 6–8 K. The magnetization dependences  $M(H)$  in magnetic fields up to 5 T appeared to be close to linear, indicating that the concentrations of ferromagnetic impurities are negligibly small. A typical temperature dependence of the magnetic susceptibility for single-crystal FeSe samples is shown in figure 2. As is seen, a substantial growth of

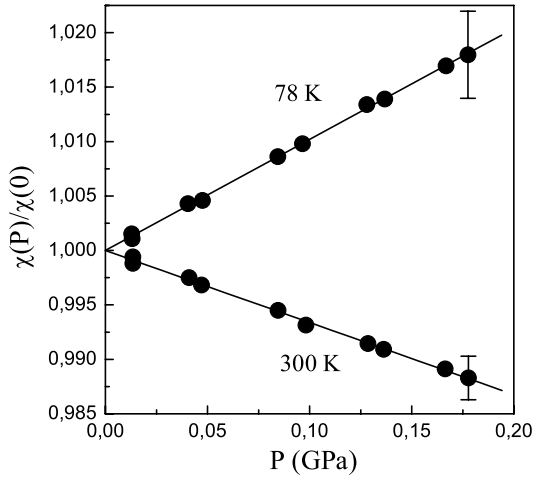


**Figure 3.** Pressure dependences of the magnetic susceptibility, normalized to its value at  $P = 0$ , for the polycrystalline FeSe compound at temperatures 78 and 300 K. The solid lines are guides for the eye.

susceptibility with temperature was revealed in the normal state, as well as a large magnetic anisotropy. The upturn of susceptibility at  $T \rightarrow 0$  (low temperature ‘tail’) is presumably related to a small amount of magnetic impurities in our samples.

The study of magnetic susceptibility of FeSe under helium gas pressure  $P$  up to 0.2 GPa was performed at fixed temperatures 78 and 300 K using a pendulum-type magnetometer placed directly in the nonmagnetic pressure cell [25]. In order to measure the pressure effect with a reasonable accuracy, a sufficiently large mass of the sample is required. We have used an FeSe sample, further called ‘polycrystalline’ FeSe, which was prepared by compacting a number of about 50 of small arbitrarily oriented single crystals inside an aluminum foil cylinder. The total mass of the sample was about 200 mg. The measurements were carried out in a field  $H = 1.7$  T and their relative errors did not exceed 0.5%. The experimental pressure dependences  $\chi(P)$  at different temperatures are shown in figure 3, which demonstrates their linear character. The negative value of the pressure effect,  $d \ln \chi/dP \simeq -6.5 \times 10^{-2} \text{ GPa}^{-1}$ , was observed at temperature 300 K, whereas at  $T = 78$  K the effect appeared to be positive,  $d \ln \chi/dP \simeq 10 \times 10^{-2} \text{ GPa}^{-1}$ . The available experimental and theoretical results on  $d \ln \chi/dP$  for FeSe are compiled in table 1 together with corresponding data for the relative FeTe compound for comparison.

### 3. Computational details and results

In order to analyze the magnetic properties of the FeSe compound in the normal state, *ab initio* calculations of the electronic structure and paramagnetic susceptibility were carried out. At ambient conditions the FeSe compound possesses the tetragonal PbO-type crystal structure (space group  $P4/nmm$ ), which is composed by alternating triple-layer slabs. Each iron layer is sandwiched between two nearest-neighbor layers of Se, which form edge-shared

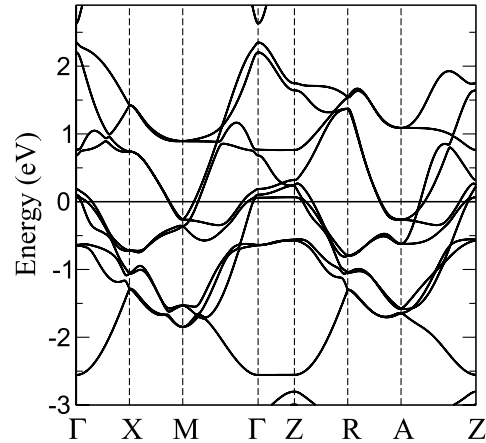


**Figure 4.** Band structure of FeSe around the Fermi level (at 0 eV) marked by a horizontal line.

**Table 1.** Pressure derivatives of the magnetic susceptibility  $d \ln \chi/dP$  (in units  $10^{-2} \text{ GPa}^{-1}$ ) for FeSe and FeTe compounds at different temperatures.

	$T$ (K)	$d \ln \chi/dP$	
		FeSe	FeTe <sup>a</sup>
Experiment	300	$-6.5 \pm 1$ $\sim -7^b$	$13 \pm 1$
	78	$10 \pm 3$ $\sim 6.5^b$	$23 \pm 1.5$
	20	$\sim 9^b$	
Theory	0	$\simeq 8$	$\sim 20$

<sup>a</sup> Results for FeTe are taken from [26].

<sup>b</sup> From NMR Knight shift data of [20].

tetrahedra around the iron sites. The positions of selenium layers are fixed by the structural parameter  $Z$ , which represents the relative height of Se atoms above the iron plane. The structural parameters of FeSe were determined by means of x-ray and neutron diffraction [3, 6, 7, 9, 14, 27].

The main purpose of the present *ab initio* calculations was to evaluate the paramagnetic response in an external magnetic field and to elucidate the nature and features of magnetism in the normal state of the FeSe compound. In the context of this task, the dependences of the magnetic susceptibility on volume, lattice parameters and temperature were addressed. *Ab initio* calculations of the electronic structure of FeSe were performed by employing a full-potential all-electron relativistic linear muffin-tin orbital method (FP-LMTO, code RSPt [28, 29]). The exchange–correlation potential was treated within the local-spin-density approximation (LSDA) [30] of the DFT. The calculated basic features of the electronic structure of FeSe appeared to be in a qualitative agreement with results of previous DFT calculations [31–34].

As is seen in figures 4 and 5, the calculated band structure and density of electronic states (DOS) of FeSe indicate the presence of the hybridized predominantly d-like Fe electronic states close to the Fermi level  $E_F$ . The chalcogen p-states are situated well below  $E_F$  and slightly hybridized with the

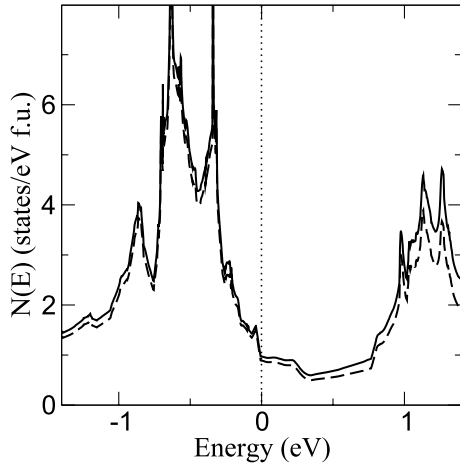


**Figure 5.** Total density of electronic states of FeSe (solid line) and the partial contribution of the iron d-states (dashed line). The Fermi level position at 0 eV is marked by a vertical line.

d-states of iron. Also, one can see a van Hove singularity in figure 5 at  $\sim 40$  meV below  $E_F$ . It should be noted, that a proximity of the van Hove singularity to the Fermi level is considered as the key ingredient for superconductivity in iron-based superconductors [35].

To evaluate the paramagnetic susceptibility of FeSe, the FP-LMTO-LSDA calculations of field-induced spin and orbital (Van Vleck) magnetic moments were carried out within the approach described in [36]. The relativistic effects, including spin-orbit coupling, were incorporated, and the effect of an external magnetic field  $\mathbf{H}$  was taken into account self-consistently by means of the Zeeman term:

$$\mathcal{H}_Z = \mu_B \mathbf{H} \cdot (2\hat{\mathbf{s}} + \hat{\mathbf{l}}). \quad (1)$$

Here  $\mu_B$  is the Bohr magneton,  $\hat{\mathbf{s}}$  and  $\hat{\mathbf{l}}$  are the spin and orbital angular momentum operators, respectively. The field-induced spin and orbital magnetic moments provide estimations of the related contributions to the magnetic susceptibility,  $\chi_{\text{spin}}$  and  $\chi_{\text{orb}}$ . For the tetragonal crystal structure the components of these contributions,  $\chi_{i\parallel}$  and  $\chi_{i\perp}$ , are derived from the magnetic moments calculated in the external field, which was applied parallel and perpendicular to the  $c$  axis, respectively.

It is found that magnetic response to the external field is very sensitive to the unit cell volume, as well as to the structural parameter  $Z$ , which represents the relative height of chalcogen species from the Fe plane. The calculated dependences of susceptibility of FeSe as functions of the volume and parameter  $Z$  are given in figures 6 and 7, respectively. The theoretical unit cell volume in figure 6 was determined as corresponding to the minimum of the calculated volume dependence of the total energy  $E(V)$ , whereas the experimental volume corresponds to XRD measurements on our sample at room temperature (figure 1).

Also, the thermal effects are taken into account in order to calculate the temperature dependence of paramagnetic susceptibility for the FeSe compound. In this case the field-induced spin and orbital magnetic moments were evaluated by corresponding integration with the energy

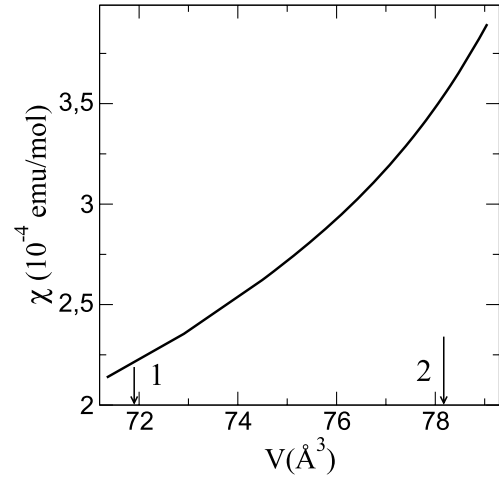


**Figure 6.** Calculated paramagnetic susceptibility of FeSe as a function of the unit cell volume (in  $\text{\AA}^3$ ).  $Z$  is taken to be 0.26. The arrows indicate the theoretical (1) and experimental (2) equilibrium volume values.

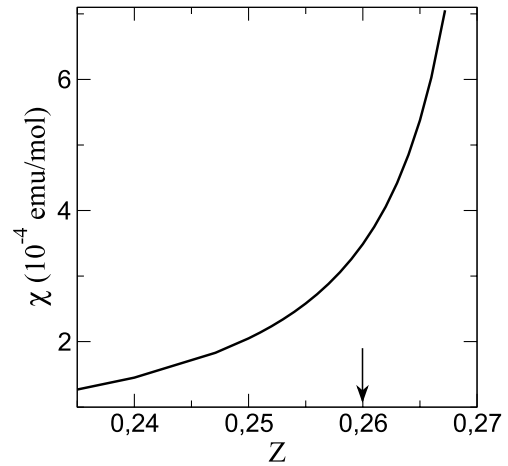


**Figure 7.** Calculated paramagnetic susceptibility of FeSe as a function of internal parameter  $Z$  for the experimental unit cell volume. The arrow indicates the experimental value of  $Z$ .

derivative of the Fermi-Dirac distribution function  $f(E, \mu, T)$ , and the temperature dependence of  $\chi$  was actually determined by taking into account the finite width of  $-df/dE$  (see [29] for details). It should be noted that the energy derivative of the Fermi-Dirac distribution corresponds to a Dirac delta function at low temperatures, having a sharp positive peak at the Fermi energy  $E_F$ . This steep behavior of  $-df/dE$  resulted in some instability in the numerical calculations of  $\chi$ , which are seen in figure 8.

#### 4. Discussion

The experimental superconducting transition temperatures 6–8 K, obtained for the studied  $\text{FeSe}_{1-x}$  samples, agree with those reported in the literature [1, 3–6]. Above  $T_c$ , a substantial growth of susceptibility with temperature is revealed in the normal state of FeSe up to 300 K (figure 2),

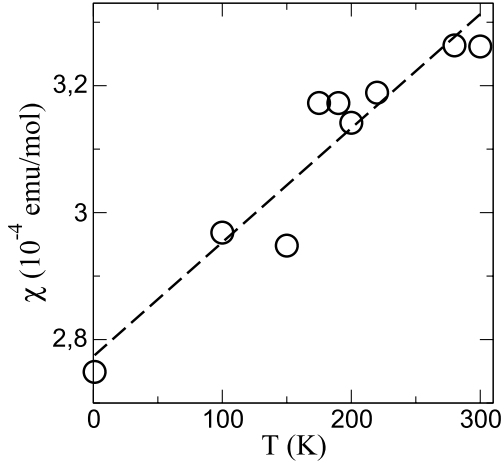


**Figure 8.** Calculated temperature dependence of the paramagnetic susceptibility of FeSe.  $Z$  is taken to be 0.26, the unit cell volume is fixed between the theoretical and experimental values. The dashed line is a guide for the eye.

which indicates the itinerant nature of electronic states of Fe at the Fermi energy.

The total susceptibility in the absence of spontaneous magnetic ordering can be represented as the sum:

$$\chi_{\text{tot}} = \chi_{\text{spin}} + \chi_{\text{orb}} + \chi_{\text{dia}} + \chi_{\text{L}}, \quad (2)$$

where these terms correspond to the Pauli spin susceptibility, a generalization of the Van Vleck orbital paramagnetism, the Langevin diamagnetism of closed ion shells, and a generalization of Landau conduction electrons diamagnetism, respectively. Obviously, the  $\chi_{\text{dia}}$  term does not provide any anisotropy, and for FeSe the Langevin diamagnetism of closed ion shells can be estimated according to [37] as  $\chi_{\text{dia}} \simeq -0.2 \times 10^{-4} \text{ emu mol}^{-1}$ .

In order to analyze the experimental data on  $\chi$  for FeSe we used the calculated paramagnetic contributions to susceptibility,  $\chi_{\text{spin}}$  and  $\chi_{\text{orb}}$ . It has been shown [36] that for paramagnetic metallic systems the Stoner approach underestimates the spin susceptibility, whereas the LSDA field-induced calculations take into account non-uniform-induced magnetization density and provide a more adequate description. The present field-induced calculations of the paramagnetic susceptibility for FeSe revealed that this system is in close proximity to the magnetic critical point. This can be seen from a steep rise of  $\chi(V)$  and  $\chi(Z)$  in figures 6 and 7, respectively, above the corresponding experimental values of  $V$  and  $Z$ . In fact, the calculated Stoner enhancement  $S \sim 7$  (see [31]) also indicates that FeSe is close to the ferromagnetic Stoner instability.

For the unit cell volume chosen between the theoretical and experimental values, the dominant spin contribution to magnetic susceptibility of FeSe is estimated to be  $\chi_{\text{spin}} \simeq 2.4 \times 10^{-4} \text{ emu mol}^{-1}$ . The averaged orbital  $\chi_{\text{orb}}$  term amounts to  $\sim 0.4 \times 10^{-4} \text{ emu mol}^{-1}$ , being about 15% of the total paramagnetism. From comparison of the calculated paramagnetic susceptibility for the ground state in figure 8,  $\chi_{\text{para}} = \chi_{\text{spin}} + \chi_{\text{orb}} \simeq 2.8 \times 10^{-4} \text{ emu mol}^{-1}$ , with the

experimental value  $\chi_{\text{exp}}$  at  $T \rightarrow 0 \text{ K}$  in figure 2,  $\chi_{\text{exp}} = (\chi_{\parallel} + 2\chi_{\perp})/3 \simeq 1.5 \times 10^{-4} \text{ emu mol}^{-1}$ , it is clear that calculated value  $\chi_{\text{para}}$  has to be substantially compensated by a diamagnetic contribution in order to conform with the experimental data. One can estimate the expected diamagnetic contribution to magnetic susceptibility of FeSe to be about  $(\chi_{\text{exp}} - \chi_{\text{para}}) \sim -1.3 \times 10^{-4} \text{ emu mol}^{-1}$ . This diamagnetism is comparable in absolute value to the paramagnetic contribution, being much larger than the above-estimated Langevin diamagnetism  $\chi_{\text{dia}}$ . Apparently, it can be ascribed to the  $\chi_{\text{L}}$  term in equation (2).

According to the experimental data in figure 2, the observed anisotropy of susceptibility  $\Delta\chi$  is large in FeSe, and even comparable to the averaged susceptibility itself at low temperatures. It appears to be much larger than the calculated anisotropy of the orbital contribution to paramagnetic susceptibility of FeSe,  $\Delta\chi_{\text{orb}} = \chi_{\text{orb}\parallel} - \chi_{\text{orb}\perp} \simeq -0.1 \times 10^{-4} \text{ emu mol}^{-1}$ . Therefore, in order to explain the experimental  $\Delta\chi$  one can assume the presence of a substantial and presumably anisotropic diamagnetic contribution from conduction electrons.

To calculate the Landau diamagnetic contribution  $\chi_{\text{L}}$  is a rather difficult problem [38, 39]. The free-electron Landau approximation, which is often used for estimations, provides  $\chi_{\text{L}}^0$  that equals  $-\frac{1}{3}$  of the Pauli spin susceptibility. However, for many metallic systems the diamagnetism of conduction electrons  $\chi_{\text{L}}$  can be many times larger than the free-electron Landau estimate  $\chi_{\text{L}}^0$ , and such anomalous and anisotropic diamagnetism is often determined by the presence of quasi-degenerated states with small effective masses at  $E_{\text{F}}$  (see [39] and references therein). As can be seen in figure 4, in FeSe the quasi-degenerate states with small effective masses exist at  $E_{\text{F}}$  around the symmetry points  $\Gamma$  and  $Z$ , where the band degeneracies are lifted by the spin-orbital coupling. Such band structure features are of particular importance in connection with a manifestation of the anomalously large and anisotropic  $\chi_{\text{L}}$ , which was found to originate from the similar degeneracy points [39]. It should be emphasized that rigorous theoretical analysis of  $\chi_{\text{L}}$  is a rather cumbersome procedure, which goes beyond the aims of the present work. At this stage, we have identified appropriate electronic states near  $E_{\text{F}}$  as possible sources of the large and anisotropic conduction electrons diamagnetism in FeSe.

The theoretically evaluated temperature dependence of the paramagnetic susceptibility  $\chi_{\text{para}}(T)$  in figure 8, which takes into account the finite width of the energy derivative of the Fermi-Dirac distribution function, actually provides only a slight increase in  $\chi$  with temperature. Thus, the observed substantial growth of  $\chi(T)$  is rather puzzling at present. It is presumably related to a fine structure of the DOS at  $E_{\text{F}}$ , but one should expect that FeSe system is driven far from the ground state at room temperatures. At this stage, we should admit that increase of the unit cell volume for the tetragonal  $P4/nmm$  phase ( $\Delta V/V \simeq 1\%$  with temperature rising up to 300 K, see [12]) can provide about 10% growth of paramagnetic susceptibility, according to the  $\chi(V)$  dependence in figure 6. However, this volume expansion does not explain the experimental

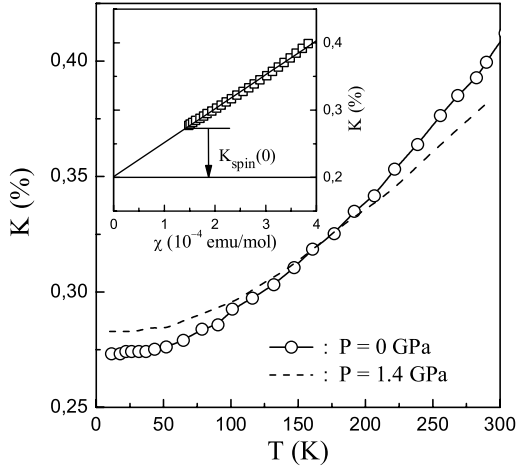


**Figure 9.** Temperature dependences of the NMR Knight shift  $K$  in FeSe measured at ambient pressure ( $\circ$ ) and at  $P = 1.4$  GPa (dashed line). The data are taken from [20]. The inset shows the dependence of  $K$  on the averaged magnetic susceptibility for FeSe,  $\chi = (\chi_{\parallel} + 2\chi_{\perp})/3$ , from figure 2.

$\chi(T)$  in figure 2. Also, a change of the structural parameter  $Z$  with temperature can be substantial and of importance due to the strong  $\chi(Z)$  dependence in figure 7, but to date the influence of temperature on  $Z$  has not been studied in a systematic way. Therefore, noticeable temperature effects on the lattice parameters, chalcogen atom position  $Z$ , and electronic structure itself should be taken into account in a rigorous quantitative analysis of  $\chi(T)$  in FeSe.

The measured pressure effects on the magnetic susceptibility of FeSe are intriguing and require a detailed examination. Firstly, as can be seen in table 1, there is a striking sign difference for the pressure effects on  $\chi$  at low and room temperatures. Also, the absolute value of this effect is substantially larger than that observed in strongly enhanced itinerant paramagnets [36], and appeared to be comparable with such pressure effect on  $\chi$  reported for the related FeTe compound [26] (see table 1).

It should be noted that the present experimental data on  $\chi(T, P)$  for FeSe are in reasonable agreement with the results of [20] on temperature and pressure dependences of the NMR Knight shift  $K$  of FeSe in the normal state. As can be seen in figure 9, the temperature dependence  $K(T)$  at ambient pressure reflects the corresponding dependence of the magnetic susceptibility in figure 2. Assuming the latter to be governed by the spin susceptibility  $\chi_{\text{spin}}(T)$ , the only temperature-dependent contribution in  $K(T)$  can be determined as  $K_{\text{spin}}(T) = \alpha \chi_{\text{spin}}(T)$  with  $\alpha \simeq 5 \times 10^2 \text{ \%}(\text{emu mol}^{-1})^{-1}$ , resulting from the slope of  $K$  versus  $\chi$  linear dependence in the inset of figure 9. In addition, this contribution is expected to be also responsible for the pressure effect on  $K$ . Using a rough approximation,  $\chi_{\text{spin}}(T) \approx \chi(T)$ , we obtain an estimate of  $d \ln \chi / dP \approx d \ln K_{\text{spin}} / dP$ , which is listed in table 1.

In order to clarify the behavior of  $\chi(P)$  in FeSe, we carried out the *ab initio* calculations of paramagnetic susceptibility as a function of pressure. These calculations

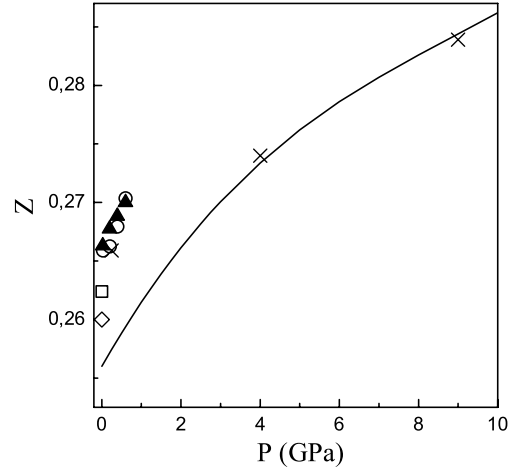


**Figure 10.** Pressure dependence of the internal chalcogen structural parameter  $Z$  for FeSe. The solid line indicates the results of calculations from [34]. Experimental data on the parameter  $Z$  in FeSe for the tetragonal phase at  $T = 190$  K ( $\blacktriangle$ , [7]),  $T = 295$  K ( $\square$ , [27]),  $T = 300$  K ( $\diamond$ , [9]), and for the orthorhombic phase at  $T = 16$  K ( $\times$ , [3]) and  $T = 50$  K ( $\circ$ , [7]).

are based upon the pressure-dependent structural parameters, which have been calculated and listed in [34]. As is seen in figure 10, the calculated behavior of  $Z(P)$  follows the available experimental data [3, 7, 9, 14, 27]. In the course of corresponding calculations of  $\chi(P)$  for FeSe we evaluated the pressure derivative  $d \ln \chi / dP \simeq 8 \times 10^{-2} \text{ GPa}^{-1}$  in the range 0–1 GPa. The evaluated derivative appeared to be in a qualitative agreement with the experimental low-temperature data (see table 1).

As part of these electronic structure calculations for FeSe, we also obtained a pressure dependence of the density of states at the Fermi level, which is presented in figure 11. In addition to the calculated structural parameters from [34], we also employed the small upward shift  $\Delta Z = +0.004$  to start the optimized  $Z(P)$  dependence from the experimental value  $Z = 0.26$  (see  $Z(P)$  behavior in figure 10). The corresponding two sets of calculations demonstrate in figure 11 a tolerable variation of  $N(E_F)$  behaviors in FeSe under pressure, depending on a small adjustment of  $Z(P = 0)$  between the theoretical and experimental values.

With the aim to elucidate the main mechanism of the experimentally observed strong increase of the magnetic susceptibility of FeSe under pressure at low temperatures, we have also analyzed the pressure effect in terms of the corresponding changes of the volume and  $Z$  parameters by using the relation:

$$\frac{d \ln \chi}{dP} = \frac{\partial \ln \chi}{\partial \ln V} \times \frac{d \ln V}{dP} + \frac{\partial \ln \chi}{\partial Z} \times \frac{dZ}{dP}. \quad (3)$$

The required values of the partial volume and  $Z$  derivatives of  $\chi$  can be estimated from the results of *ab initio* calculations presented in figures 6 and 7, and were found to be  $\partial \ln \chi / \partial \ln V \simeq 8$  and  $\partial \ln \chi / \partial Z \simeq 65$  for values of  $V$  and  $Z$  close to the experimental data. The optimized value  $d \ln V / dP = -3 \times 10^{-2} \text{ GPa}^{-1}$  is taken for the compressibility of FeSe [34]. This calculated compressibility agrees closely

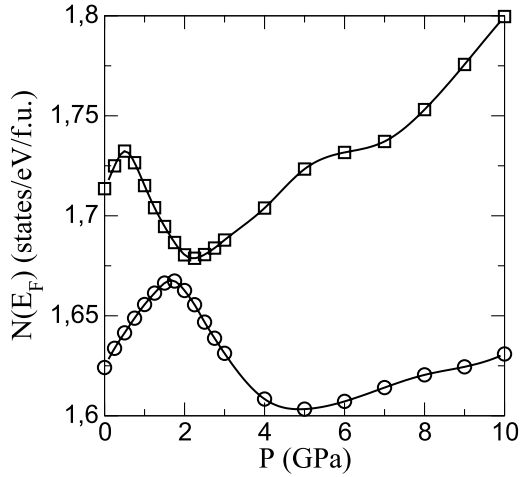


**Figure 11.** Calculated pressure dependences of the density of states at the Fermi level for FeSe. The pressure-dependent structural parameters, including the lattice constants and chalcogen atom position  $Z$ , were taken from the calculations of [34] (○). For another set of  $N(E_F)$  calculations (□) the small upward shift  $\Delta Z = +0.004$  was employed to start from the experimental value  $Z = 0.26$  (see  $Z(P)$  behavior in figure 10). The solid lines are guides for the eye.

with the experimental values  $-3.1 \pm 0.1 \times 10^{-2} \text{ GPa}^{-1}$  [4, 7, 13]. Also, the optimized value  $dZ/dP \simeq 0.55 \times 10^{-2} \text{ GPa}^{-1}$  was adopted for evaluation of equation (3). As is seen in figure 10, this value of  $dZ/dP$  is in agreement with the experimental data at low pressures. As far as all parameters entering equation (3) are estimated, the first term in (3) results in a large negative value  $\partial \ln \chi / \partial \ln V \times d \ln V / dP \simeq -24 \times 10^{-2} \text{ GPa}^{-1}$ , whereas the second term appears to be large and positive:  $\partial \ln \chi / \partial Z \times dZ / dP \simeq 36 \times 10^{-2} \text{ GPa}^{-1}$ . Both the terms in equation (3) taken together yield the estimate  $d \ln \chi / dP \simeq 12 \times 10^{-2} \text{ GPa}^{-1}$  for FeSe, which is consistent with the low-temperature experimental data. This estimate is also close to the *ab initio* calculated pressure derivative based on theoretical lattice parameters from [34] ( $d \ln \chi / dP \simeq 8 \times 10^{-2} \text{ GPa}^{-1}$ , see table 1). Actually, the difference in these evaluated values of  $d \ln \chi / dP$ , depending on whether experimental or theoretical lattice parameters are employed, covers a reasonable range for the expected pressure effect on  $\chi$ .

Based on the results of calculations, presented in figures 6 and 7, the observed hydrostatic pressure effect on  $\chi$  in FeSe at low temperatures can be represented as a sum of two large competing contributions, related to the pressure dependence of the structural parameters  $V$  and  $Z$ . As a result, the experimental positive value of the pressure effect,  $d \ln \chi / dP \simeq 10 \times 10^{-2} \text{ GPa}^{-1}$ , is determined by the dominating contribution from the change of  $Z$  under pressure.

Actually, the nature of the large positive pressure effect on  $\chi$  in FeSe is similar to that reported for the FeTe compound [26]. However, in the case of FeTe such an effect is twice as pronounced, and also takes place at room temperatures, whereas for FeSe  $d \ln \chi / dP$  is found to be negative at 300 K (see table 1). The reason for this difference is unclear and has still to be elucidated. At the present stage

one can presume that the negative sign of the  $d \ln \chi / dP$  derivative is probably related to the nature of the observed anomalous growth of  $\chi(T)$  up to room temperatures (figure 2), which is not the case for FeTe [26]. It appears that at higher temperatures this anomalous growth of  $\chi(T)$  in FeSe is apparently reduced by applied pressure.

Basically, the observed positive pressure effect on  $\chi$  in FeSe at low temperatures correlates with the calculated increase of the density of states at the Fermi level  $N(E_F)$  at low pressures (see figure 11). At higher pressures one can see a nonmonotonic variation of  $N(E_F)$  in figure 11, which clearly exhibits consecutive maximum and minimum. It was recently shown [40] that superconducting transition temperatures  $T_c$  of a number of iron-based superconductors correlate with the corresponding values of the density of states at the Fermi level, thus supporting the BCS-like pairing mechanism in these systems. Remarkably, the presently calculated behavior of  $N(E_F)$  under pressure (the upper curve in figure 11, with a maximum at 0.5 GPa and a minimum at 2.2 GPa) is qualitatively consistent with the reported experimental dependences of  $T_c(P)$  in FeSe (corresponding maximum and minimum of  $T_c(P)$  were observed at  $P \simeq 0.8 \text{ GPa}$  and  $P \simeq 1.2 \text{ GPa}$ , respectively [17, 18, 21, 22]). The calculated pressure dependence of the DOS at the Fermi level for FeSe with the structural parameters taken from [34] (the lower curve in figure 11) also contains consecutive maximum and minimum of  $N(E_F)$  which are substantially shifted to higher pressures.

## 5. Conclusions

The magnetic susceptibility of the FeSe compound is found to rise substantially with temperature, which apparently points to the itinerant nature of the electronic states of Fe. The calculated paramagnetic susceptibility  $\chi_{\text{para}}(T)$  describes qualitatively the experimental dependence  $\chi(T)$ , however the origin of the observed approximately twofold increase of  $\chi$  up to 300 K is puzzling. From comparison of the experimental values of susceptibility and its anisotropy with that calculated for paramagnetic contributions to  $\chi$  in FeSe, the additional anisotropic diamagnetism is expected to be of the order of  $-1 \times 10^{-4} \text{ emu mol}^{-1}$ , which can relate to the diamagnetism of conduction electrons and presumably has its origin in the quasi-degenerate electronic states close to  $E_F$ .

The measurements of magnetic susceptibility under hydrostatic pressure revealed a strong positive effect at low temperatures. This effect appeared to be comparable to that reported for the related FeTe compound [26], whereas at room temperature the pressure effect for FeSe is also found to be strong, but *negative*.

Our calculations indicate that the paramagnetic susceptibility of the FeSe compound is substantially dependent on the unit cell volume  $V$  and the relative height  $Z$  of Se species above the Fe plane. It is shown that the large positive pressure effect on  $\chi$  observed at low temperatures is related to the strong sensitivity of the paramagnetic susceptibility to the parameter  $Z$ , which determines the dominant positive contribution. The origin of the negative sign of the  $d \ln \chi / dP$

derivative in FeSe at 300 K is unclear and probably linked to the nature of the observed anomalous growth of  $\chi(T)$ . At present one can state that at higher temperatures this anomalous growth of  $\chi(T)$  in FeSe is apparently reduced by applied pressure.

The present *ab initio* calculations have demonstrated that for FeSe compound the nonmonotonic behavior of the superconducting transition temperature with pressure qualitatively correlates with the density of electronic states at the Fermi level. This indicates a possible realization of the BCS-like pairing mechanism in this system.

## Acknowledgments

This work was supported by the Russian–Ukrainian RFBR–NASU projects 01-02-12 and 12-02-90405, by the Russian Ministry of Science and Education through state contracts 11.519.11.6012 and 14.740.11.1365, and government contract 8378, by the NASU Young Scientists Grant 03-2012, and by a grant of the President of the Russian Federation for State Support of Young Russian Scientists (MK-1557.2011.5).

## References

- [1] Hsu F C *et al* 2008 *Proc. Natl Acad. Sci. USA* **38** 14262
- [2] Medvedev S *et al* 2009 *Nature Mater.* **8** 630
- [3] Margadonna S, Takabayashi Y, Ohishi Y, Mizuguchi Y, Takano Y, Kagayama T, Nakagawa T, Takata M and Prassides K 2009 *Phys. Rev. B* **80** 064506
- [4] Braithwaite D, Salce B, Lapertot G, Bourdarot F, Marin C, Aoki D and Hanfland M 2009 *J. Phys.: Condens. Matter* **21** 232202
- [5] McQueen T M *et al* 2009 *Phys. Rev. B* **79** 014522
- [6] Pomjakushina E, Conder K, Pomjakushin V, Bendele M and Khasanov R 2009 *Phys. Rev. B* **80** 024517
- [7] Millican J N, Phelan D, Thomas E L, Leao J B and Carpenter E 2009 *Solid State Commun.* **149** 707
- [8] Mizuguchi Y and Takano Y 2010 *J. Phys. Soc. Japan* **79** 102001
- [9] Hu R, Lei H, Abeykoon M, Bozin E S, Billinge S J L, Warren J B, Siegrist T and Petrovic C 2011 *Phys. Rev. B* **83** 224502
- [10] Lin J-Y, Hsieh Y S, Chareev D A, Vasiliev A N, Parsons Y and Yang H D 2011 *Phys. Rev. B* **84** 220507
- [11] Fedorchenko A V *et al* 2011 *Low Temp. Phys.* **37** 83
- [12] Mizuguchi Y and Takano Y 2011 *Z. Krist.* **226** 417
- [13] Garbarino G, Sow A, Lejay P, Sulpice A, Toulemonde P, Mezouar M and Nunez-Regueiro M 2009 *Europhys. Lett.* **86** 27001
- [14] Kumar R S, Zhang Y, Sinogeikin S, Xiao Y, Kumar S, Chow P, Corneliuss A L and Chen C 2010 *J. Phys. Chem. B* **114** 12597
- [15] Naghavi S S, Chadov S and Felser C 2011 *J. Phys.: Condens. Matter* **23** 205601
- [16] Rahman G, Kim I G and Freeman A J 2012 *J. Phys.: Condens. Matter* **24** 095502
- [17] Masaki S, Kotegawa H, Hara Y, Murata K, Mizuguchi Y and Takano Y 2009 *J. Phys. Soc. Japan* **78** 063704
- [18] Miyoshi K, Takaichi Y, Mutou E, Fujiwara K and Takeuchi J 2009 *J. Phys. Soc. Japan* **78** 093703
- [19] Okabe H, Takeshita N, Horigane K, Muranaka T and Akimitsu J 2010 *Phys. Rev. B* **81** 205119
- [20] Imai T, Ahilan K, Ning F L, McQueen T M and Cava R J 2009 *Phys. Rev. Lett.* **102** 177005
- [21] Bendele M, Amato A, Conder K, Elender M, Keller H, Klauss H-H, Luetkens H, Pomjakushina E, Raselli A and Khasanov R 2010 *Phys. Rev. Lett.* **104** 087003
- [22] Bendele M, Ichanow A, Pashkevich Yu, Keller L, Strassle Th, Gusev A, Pomjakushina E, Conder K, Khasanov R and Keller H 2012 *Phys. Rev. B* **85** 064517
- [23] Okamoto H 1991 *J. Phase Equilib.* **12** 383
- [24] Wen J, Xu G, Gu G, Tranquada J M and Birgeneau R J 2011 *Rep. Prog. Phys.* **74** 124503
- [25] Panfilov A S 1992 *Phys. Tech. High Press.* **2** 61 (in Russian)
- [26] Fedorchenko A V, Grechnev G E, Desnenko V A, Panfilov A S, Gnatchenko S L, Tsurkan V, Deisenhofer J, Loidl A, Volkova O S and Vasiliev A N 2011 *J. Phys.: Condens. Matter* **23** 325701
- [27] Gómez R W, Marquina V, Pérez-Mazariego J L, Escamilla R, Escudero R, Quintana M, Hernández-Gómez J J, Ridaura R and Marquina M L 2010 *J. Supercond. Novel Magn.* **23** 551
- [28] Wills J M, Alouani M, Andersson P, Delin A, Eriksson O and Grechnev A 2010 *Full-Potential Electronic Structure Method: Energy and Force Calculations with Density Functional and Dynamical Mean Field Theory* (Berlin: Springer)
- [29] Grechnev G E, Ahuja R and Eriksson O 2003 *Phys. Rev. B* **68** 64414
- [30] Barth U and von Hedin L 1972 *J. Phys. C: Solid State Phys.* **5** 1629
- [31] Subedi A, Zhang L, Singh D J and Du M-H 2008 *Phys. Rev. B* **78** 134514
- [32] Lee K-W, Pardo V and Pickett W E 2008 *Phys. Rev. B* **78** 174502
- [33] Singh D J 2009 *Physica C* **469** 418
- [34] Ciechan A, Winiarski M J and Samsel-Czekala M 2012 *Acta Phys. Pol. A* **121** 820
- [35] Kordyuk A A 2012 *Low Temp. Phys.* **38** 888
- [36] Grechnev G E 2009 *Low Temp. Phys.* **35** 638
- [37] Selwood P 1956 *Magnetochemistry* (New York: Interscience)
- [38] Grechnev G E, Fedorchenko A V, Logosha A V, Panfilov A S, Svechkarev I V, Filippov V B, Lyashchenko A B and Evdokimova A V 2009 *J. Alloys Compounds* **481** 75
- [39] Baranovskiy A E, Grechnev G E, Mikitik G P and Svechkarev I V 2003 *Low Temp. Phys.* **29** 356
- [40] Sadvorskii M V, Kuchinskii E Z and Nekrasov I A 2012 *J. Magn. Mater.* **324** 3481